Protein Engineering, Design & Selection, 2019, pp. 1–9
doi: 10.1093/protein/gzy034
Original Article

OXFORD

Original Article

A single mutation in cyclodextrin glycosyltransferase from *Paenibacillus barengoltzii* changes cyclodextrin and maltooligosaccharides production

JdlM Castillo[1,†], S. Caminata Landriel[1,†], M. Sánchez Costa[2], O.A. Taboga[3], J. Berenguer[2], A. Hidalgo[2], S.A. Ferrarotti[1], and H. Costa[1,4,*]

[1]Departamento de Ciencias Básicas, Universidad Nacional de Luján, Ruta 5 y Avenida Constitución, 6700 Luján, Buenos Aires, Argentina, [2]Centro de Biología Molecular Severo Ochoa, (CSIC-UAM), C/Nicolás Cabrera 1, 28049, Madrid, Spain, [3]Instituto de Biotecnología, Instituto Nacional de Tecnología Agropecuaria, De los Reseros y N. Repetto s/n, 1686 Hurlingham, Buenos Aires, Argentina, and [4]INEDES-CONICET, Universidad Nacional de Luján, Ruta 5 y Avenida Constitución, 6700 Luján, Buenos Aires, Argentina

[*]To whom correspondence should be addressed. E-mail: hcosta@unlu.edu.ar
[†]Both authors contributed equally to this work.
Edited By: Ronald Raines

Received 1 August 2018; Revised 5 December 2018; Editorial Decision 17 December 2018; Accepted 25 December 2018

Abstract

Cyclodextrin glycosyltransferases (CGTases) are bacterial enzymes that catalyze starch conversion into cyclodextrins, which have several biotechnological applications including solubilization of hydrophobic compounds, masking of unpleasant odors and flavors in pharmaceutical preparations, and removal of cholesterol from food. Additionally, CGTases produce maltooligosaccharides, which are linear molecules with potential benefits for human health. Current research efforts are concentrated in the development of engineered enzymes with improved yield and/or particular product specificity. In this work, we analyzed the role of four residues of the CGTase from *Paenibacillus barengoltzii* as determinants of product specificity. Single mutations were introduced in the CGTase-encoding gene to obtain mutants A137V, A144V, L280A and M329I and the activity of recombinant proteins was evaluated. The residue at position 137 proved to be relevant for CGTase activity. Molecular dynamics studies demonstrated additionally that mutation A137V produces a perturbation in the catalytic site of the CGTase, which correlates with a 10-fold reduction in its catalytic efficiency. Moreover, this mutant showed increased production of maltooligosaccharides with a high degree of polymerization, mostly maltopentaose to maltoheptaose. Our results highlight the role of residue 137 as a determinant of product specificity in this CGTase and may be applied to the rational design of saccharide-producing enzymes.

Key words: CGTase, cyclodextrins, maltooligosaccharides, *Paenibacillus*, starch

Introduction

Cyclodextrin glycosyltransferase (EC 2.4.1.19, CGTase) belongs to family 13 of glycoside hydrolases (GH13; Stam *et al.*, 2006), which act on starch and related α-glucans. CGTase is the only member of this family that catalyzes the synthesis of cyclic dextrins (cyclodextrins, CD) through intramolecular transglycosylation. This reaction consists in the cleavage of α-1,4 linkages in linear chain oligosaccharides and the subsequent transference of the new reducing end to a non-reducing end of the same chain. As other α-glucanotransferases, the enzyme also catalyzes α-1,4 intermolecular transglycosylation reactions by opening of CD and subsequent transference to non-reducing ends of acceptors (coupling) or by transferring one chain of linear oligosaccharides to another chain of linear oligosaccharides (disproportionation) (Van Der Maarel and Leemhuis, 2013). The latter reactions lead to the biosynthesis of α-1,4 linear dextrins (maltooligosaccharides, MOS) with different degrees of polymerization according to the nature of the acceptor employed (Rodríguez Gastón *et al.*, 2012). Additionally, CGTases also exhibit weak amylolytic activity (van der Veen *et al.*, 2000).

CGTases produce mixtures of cyclic and linear dextrins. CD are non-reducing oligosaccharides with a hydrophilic surface and a nonpolar cavity. The most common types are α-, β- and γ-CD which consist of 6, 7 or 8 glucose residues, respectively. These molecules can form inclusion complexes with many organic and inorganic compounds thus modifying their physical and chemical properties. Because of this feature, they are widely used in food, pharmaceutical, cosmetic and chemical industries (Kurkov and Loftsson, 2013; Li *et al.*, 2014; Basso *et al.*, 2015). In turn, MOS are a novel type of functional oligosaccharides with potential applications in food industry because of their mild sweetness, relative low osmolality, high water-holding capacity and suitable viscosity, as well as their ability to inhibit crystallization and delay the staling of bread (Pan *et al.*, 2017).

CGTases are classified according to their product specificity; consequently, they are called α-, β- and γ-CGTases according to the preferential production of one of the three major types of CD. Also, some CGTases produce mixtures of CD in similar proportions, as for example α/β-CGTases. The proportion and type of CD produced vary significantly depending on the genus, species and even among strains of CGTase-producing microorganisms. As mentioned above, all CGTases isolated so far produce a mixture of CD when they are incubated with starch, and CD purification from the reaction mixture is the main difficulty encountered during CD production. Recently, different researchers have attempted to direct the synthesis towards a single type of cyclodextrin (Li *et al.*, 2007; Wu *et al.*, 2012; Wang *et al.*, 2013) or to obtain enzymes with improved product yield and specificity (Li *et al.*, 2007; Wang *et al.*, 2013; Han *et al.*, 2014; Huang *et al.*, 2014; Xie *et al.*, 2014a; Ban *et al.*, 2015).

The catalytic site of CGTases possesses nine sugar-binding subsites, numbered from −1 to −7 (donor subsites) and +1 and +2 (acceptor subsites); the glycosidic bond cleavage occurs between subsites +1 and −1 (Uitdehaag *et al.*, 1999). It is known that the donor subsites −3, −6 and −7 contribute to CD formation (Leemhuis *et al.*, 2010; Wang *et al.*, 2016). Specific changes in residues involved in the catalytic site of the enzyme can affect enzyme-substrate interactions, thus driving the type of product obtained. This has been demonstrated for positions (as referred to *Bacillus circulans* 251 CGTase) 77 and 239 (Kelly *et al.*, 2008), 43, 137–144 and 188 (Goh *et al.*, 2009), 47 (Li *et al.*, 2009a), 93 (Rostinawati *et al.*, 2015), 89 and 372 (Li *et al.*, 2009b), 179 (Costa *et al.*, 2012), 195 (Xie *et al.*, 2014a; 2014b), 315 (Ban *et al.*, 2015), 577 (Huang *et al.*, 2014; Li *et al.*, 2016) and 100, 227 and 328 (Wang *et al.*, 2017). Nevertheless, the mechanism determining the size of the synthesized CD remains unknown. Previously, we have investigated the structural and biochemical characteristics of the α/β-CGTase from *Bacillus circulans* strain DF 9 R (Ferrarotti *et al.*, 1996; Costa *et al.*, 2015). This bacterial strain was recently reclassified as *Paenibacillus barengoltzii* by multilocus phylogenetic analyses (unpublished results). In this work, we further characterize the molecular determinants of product specificity of our α/β-CGTase by rational design and functional evaluation of mutant enzymes carrying γ-CGTase-specific residues.

Material and Methods

Material

Soluble potato starch and α-, β-, γ-CD and MOS mixture standards were obtained from Sigma Chemical Co. (MO, USA). The pET22b (+) expression vector was obtained from Novagen (Darmstadt, Germany), and the *Pfu* ultra-high-fidelity (HF) DNA polymerase was purchased from Agilent Technologies (Santa Clara, CA, USA). All other reagents for DNA manipulation, cloning and sequencing were from Thermo Fisher Scientific (San Diego, CA, USA). Cassava starch for food use was obtained from a local supplier. All other chemicals were AR-grade.

Strain and culture conditions

The *Paenibacillus barengoltzii* strain DF 9 R was isolated from rotten potatoes and deposited in the 'Colección de Cultivos Microbianos, FFyB, UBA', catalog number CCM-A-29:1290 from the World Federation for Culture Collections. The strain was cultured in a minimum saline medium with starch consisting of 15 mg/ml cassava starch, 4 mg/ml $(NH_4)_2SO_4$, 100 mM phosphate buffer pH 7.6, 0.02 mg/ml $MgSO_4$ and 0.02 mg/ml $FeSO_4$ and incubated at 37°C and 120 rpm for 48 h (Rosso *et al.*, 2002).

Multiple sequence alignment

All available CGTase genes with experimentally demonstrated CGTase activity (n = 53) were retrieved from public databases. Multiple sequence alignment was performed with ClustalX program (Thompson *et al.*, 1997) and manually adjusted. Sequences were grouped in product specificity (α-, β- α/β- or γ-CGTase) according to the Carbohydrate Active Enzymes (CAZy) database (Lombard *et al.*, 2014). The graphical Logo representation (Crooks *et al.*, 2004) was used to represent amino acid composition and frequency at each position.

Site-directed mutagenesis

Agilent Technologies QuikChange® Primer Design Program (http://www.genomics.agilent.com/primerDesignProgram.jsp) was used for primer design. The sequences of the oligonucleotides used in this work are listed in Table I. The fragment encoding the mature CGTase without its signal peptide and with its own stop codon was cloned previously between *Nco*I and *Xho*I restriction sites of pET22b (+) expression vector to obtain plasmid pET22b(+)/CGTase (Costa *et al.*, 2012). The purified plasmid (5 to 50 ng) was used as template for single site-directed mutagenesis reactions at positions 137, 144, 280 and 329. Reactions were performed by PCR with 2.5 U *Pfu* ultra-HF, 0.2 mM dNTPs, and 125 ng of each mutagenic primer in a 50-µl final volume. The amplification protocol included

Table I. Oligonucleotides used for site-directed mutagenesis of the *P. barengoltzii* CGTase gene.

Primer name	Sequence[a]	Length (mer)
A137V	CATAACATCAAAGTTATTATCGATTTTG**t**GCCGAACCATACTTCTCC	47
A137V antisense	GGAGAAGTATGGTTCGGC**a**CAAAATCGATAATAACTTTGATGTTATG	47
A144V	ACCATACTTCTCCGG**t**TTCTGAGACGCAGCC	31
A144V antisense	GGCTGCGTCTCAGAA**a**CCGGAGAAGTATGGT	31
L280A	CGCCAATGAATCGGGCATGAGT**g**CGCTGGATTTCCGT	37
L280A antisense	ACGGAAATCCAGCG**c**ACTCATGCCCGATTCATTGGCG	37
M329I	GGTCACGTTCATTGACAATCATGATAT**a**GATCGCTTCAAGCTC	43
M329I antisense	GAGCTTGAAGCGATC**t**ATATCATGATTGTCAATGAACGTGACC	43

[a]Mismatches are indicated in lower case bold.

incubation at 95°C for 1 min followed by 16 cycles at 95°C for 1 min and 55°C for 1 min, and a final extension at 72°C for 6 min. After 2 min on an ice bath, the reaction mixture was incubated with 10 U *Dpn*I for 2 h at 37°C. Then, an aliquot of the digested amplification product was used to transform 50 µl of competent *E. coli* BL21 (DE3). Recombinant cells were selected on LB medium with ampicillin (100 µg/ml), and at least ten recombinant clones were analyzed by automatized sequencing to confirm the incorporation of mutations.

Homology modeling

Homology models for wild type and mutant enzymes were obtained using Yasara Structure (Yasara Biosciences). This program uses the query sequence to search for homologous proteins in the PDB (Protein Data Bank) and provides a refined high-resolution model. The crystal structure corresponding to a CGTase from *Bacillus circulans* 251 strain (PDB code 1CXH; Knegtel *et al.*, 1995) was used as the template for modeling (total score 1496.47, resolution 2.41 Å). In this crystal structure, the enzyme contains maltotetraose molecule as enzyme substrate. Sequence identity between the CGTase from *Paenibacillus barengoltzii* and the template for homology modeling is 69.1% with 83% sequence similarity. Other homology modeling parameters, PSI-BLAST iterations, PSI-BLAST E-value, oligomerization state, alignment number per template, terminal extension and new loops were set according to Yasara default values. A final round of simulated annealing minimization in explicit solvent was performed to improve the final model. Best models were ranked based on *Z*-score value. The overall *Z*-scores for all models have been calculated as the weighted averages of the individual *Z*-scores using the following formula: overall = (0.145 × dihedrals) + (0.390 × packing1D) + (0.465 × packing3D).

Molecular dynamics simulations

All the molecular dynamics were also run with Yasara Structure using the Amber 14 force field with a cut-off for van der Waals forces at 8 Å. Parameters as temperature (298 K), pressure control (maximum density allowed for the solvent of 0.997 g/ml) and pH (7.4) were set by default. Snapshots were obtained every 100 ps for 20 ns. The resulting trajectories were analyzed in order to calculate the RMSD values, bonds, distances between atoms and cavities. The simulations were run using eight cores in the computer cluster of Centro de Computación Científica of the Universidad Autónoma de Madrid. The Pymol Molecular Graphics system, version 0.99. (Schrödinger, LLC) was used to generate images.

Purification of native and recombinant CGTases

Native CGTase (n-CGTase) from *Paenibacillus barengoltzii* was obtained and purified according to Rosso *et al.* (2002). Recombinant proteins (wild type [r-CGTase] and mutant CGTases A137V, A144V, L280A and M329I) were expressed from the pET22b(+) derivatives in *E. coli* BL21 (DE3) using the procedure described by Green *et al.* (2012) and purified from the periplasm as described previously (Li *et al.*, 2010). Briefly, 200 ml cultures of *E. coli* BL21 (DE3) transformed with the corresponding expression plasmids were grown for 18 h at 37°C in the presence of isopropyl 0.4 mM β-D-thiogalactoside (IPTG). Cells were harvested by centrifugation for 20 min at 20 000 × g and 4°C, and the pellets were resuspended in cold 30 mM Tris–HCl pH 7.0 with 250 mg/ml sucrose and 1 mM EDTA. The mixture was then stirred for 2 h at 200 rpm and 4°C and centrifuged for 20 min at 20 000 × *g* and 4°C. Finally, the supernatant was subjected to affinity chromatography with a column prepared with Sepharose 4B, activated with divinyl sulfone and derivatized with α-CD according to the modified method of Porath and Ersson, 1973 (Ferrarotti *et al.*, 1996).

SDS-PAGE electrophoresis

Protein concentration was determined according to Bradford (1976) with bovine serum albumin as the standard. Sodium dodecyl sulfate-polyacrylamide gel electrophoresis (SDS-PAGE) was performed according to Laemmli (1970).

Peptide sequencing

The N-terminal sequencing of each recombinant CGTase was carried out at the Facility for Peptide and Protein Sequencing (Universidad de Buenos Aires) with a Procise 492 Applied Biosystems sequencer. Phenylthiohydantoin amino acids were identified by using an online reverse-phase high-performance liquid chromatography (HPLC) system. Four cycles of Edman degradation were performed.

β-CD formation and amylolytic activities

The enzymatic formation of β-CD (β-cyclizing activity) was measured by the phenolphthalein method (Goel and Nene, 1995), employing 20 mg/ml soluble potato starch as the substrate in 50 mM Tris-HCl buffer, pH 7.0, at 55°C. One unit of CGTase is defined as the amount of enzyme catalyzing the production of 1 µmol of β-CD per min under the reaction conditions. Amylolytic activity was determined by a modification of the method of Fuwa (Rosso *et al.*, 2002), recording the reduced intensity of blue color of starch-iodine complex in the presence of the active enzyme at 660 nm. One unit of amylolytic activity (U) is defined as the amount

of enzyme that produces a difference of absorbance of 1.0 per min. Experiments were performed in triplicate.

Determination of kinetic parameters

Aliquots of 1 ml gelatinized soluble potato starch solutions (0.1 to 15.0 mg/ml) in 25 mM phosphate buffer pH 6.4 were incubated with 10 µl (1,2 µg) of purified native or recombinant CGTase, 5 U/g of starch, at 55°C. The initial rate of β-CD production was determined by the phenolphthalein method (Goel and Nene, 1995) and the results were analyzed by means of Lineweaver–Burk plots to obtain K_m and V_{max} values (GraphPadPrism version 7.00 software, San Diego, CA, USA). The turnover number (k_{cat}) was determined by dividing the value of V_{max} by the enzyme concentration used in the analysis ($k_{cat} = V_{max}/[E]_0$). Experiments were performed in triplicate.

Production of CD and MOS from starch

To study the CD obtained from starch, the experimental conditions were reproduced from Szerman *et al.* (2007). Cassava starch (50 mg/ml) was incubated in sodium phosphate buffer pH 6.4 with 1.2 µg of enzyme per gram of substrate during 4 h at 56°C and 100 rpm. For MOS production, the above reaction mixture was supplemented with 50 mg/ml glucose and incubation lasted for 24 h at 56°C and 100 rpm (Rodríguez Gastón *et al.*, 2012). The enzyme was inactivated by treatment at 100°C for 5 min. The reaction mixtures were centrifuged for 15 min at 16 000× *g* and the supernatants were ultrafiltered through Amicon YM10 membranes (cut-off 10 kDa). The oligosaccharides were analyzed by HPLC using a Könik KNK-500 apparatus, with a Restek Pinnacle II Amino 5 µm 250 × 4.6 column for carbohydrate analysis at 25°C. Samples (100 µl, 10-50 mg carbohydrate/ml) were injected. Standard solutions of known concentration of α-, β-, γ-CD and MOS (M2 to M7) were used for quantification. CD and MOS were eluted with acetonitrile/water (60:40) at a flow rate of 1.0 ml/min. For detection, a differential refractometer RID-10A-Shimadzu was used and the oligosaccharides concentration was determined by comparison of the areas under the curve of signals from the samples and the standards used. All analyses were performed in triplicate in three independent experiments.

Statistical analysis

Statistical analyses were performed using GraphPadPrism version 7.00 software (San Diego, CA, USA). Significant differences between means were calculated using one-way analysis of variance (ANOVA) followed by a Tukey *a posteriori* test. Statistical significance was considered when $P < 0.05$.

Results

Selection and production of mutant CGTases

In order to identify determinants of product specificity of CGTases, the amino acid sequences of all the CGTases from bacteria and archaea described so far ($n = 53$) were aligned and grouped by their product specificity according to the CAZy database in α- ($n = 9$), β- ($n = 33$), α/β- ($n = 8$) and γ-CGTases ($n = 3$) (Supplementary Figure S1). In particular, conservation of residues at positions that interact with the catalytic site within each type of CGTase was investigated. As illustrated in Figure 1 and Supplementary Figure S1, at position 137 all γ-CGTases possess valine, as do β-CGTase from archaea *Thermococcus kodakaraensis* and α-CGTases from the archaea *Haloferax mediterranei* and *Thermococcus* sp. In contrast, A137 is the most frequent residue in α-, β- and α/β-CGTases. In turn, at position 144 all γ-CGTases and the β-CGTase from archaea *T. kodakaraensis* show a valine residue, whereas A144 is the major residue in most other enzymes. On the other hand, all γ-CGTases contain alanine at position 280 while leucine is present at this position in all α- and α/β- CGTases and most β-CGTases. Finally, at position 329 γ-CGTases contain isoleucine, while methionine is the only amino acid present in α/β-CGTases or the most abundant residue for α- and β-CGTases. Together, this study suggests a putative role of residues 137, 144, 280 and 329 in product specificity. Noteworthy, these positions have not been analyzed individually previously, despite the fact that they interact with the binding subsites of the catalytic site of the enzyme (Supplementary Figure S1).

Single mutations at the selected positions were incorporated into the CGTase-coding sequence from *P. barengoltzii* strain DF 9 R (r-CGTase) to obtain four recombinant enzymes with mutations A137V, A144V, L280A or M329I. The enzymes were expressed from plasmid pET22b(+) in *E. coli* BL21 (DE3). This vector contains the PelB signal peptide which directs the recombinant CGTase to the periplasmic space where endopeptidases eliminate it. For protein overproduction, expression was carried out for 18 h with 0.4 mM IPTG. The periplasmic content of the cultures was obtained as described in Material and Methods section and its protein content was analyzed by SDS-PAGE (Costa *et al.*, 2012). The molecular weight of the purified recombinant proteins was indistinguishable from that of the native CGTase (n-CGTase), around 74 kDa (Supplementary Figure S1). In order to determine whether processing of the signal peptide was adequate, the amino terminus of purified recombinant CGTases was sequenced. In all cases, the sequence ^{1}MAPD^{4} was obtained, indicating that the signal peptide cleavage occurred at the right place.

Amylolytic and β-cyclizing activities of CGTases

The amylolytic activity profiles for n-CGTase, r-CGTase and mutants A137V, A144V, L280A and M329I showed no differences among enzymes except for A137V (Figure 2a). In fact, the mutation at position 137 caused a drastic decrease in starch hydrolysis (266.4 and 42.3 U/mg for mutant A137V and r-CGTase, respectively, $P < 0.0001$). Also, a significant reduction in β-cyclizing activity was observed for mutant A137V (28.8 versus 127.8 µmol β-CD/min*mg for r-CGTase, $P < 0.0001$) (Figure 2b). Therefore, this position appears to be essential for both amylolytic and β-cyclizing activities.

The kinetic parameters of the β-cyclizing reaction of native and recombinant CGTases are shown in Table II. The K_m values observed for mutant enzymes did not differ from the ones calculated for n- and r-CGTases. In addition, the catalytic efficiency (k_{cat}/K_m) of mutants A144V and M329I was similar to that of non-mutant enzymes. Conversely, mutant L280A displayed a ~30% reduction in its catalytic efficiency as compared to r-CGTase ($P < 0.05$), while in mutant A137V this decrease reached ~90% ($P < 0.0001$). These results strongly suggest a critical role of A137 and also of L280 in the β-cyclizing activity of the CGTase from *P. barengolztii*.

Production of CD and MOS

To further evaluate the impact of single mutations at positions 137, 144, 280 and 329 on CD and MOS production, both types of oligosaccharides were quantified by HPLC as described in Material and Methods. As shown in Figure 3 and Table III, mutant A137V was the only enzyme showing a decrease in total CD production (11.3 and

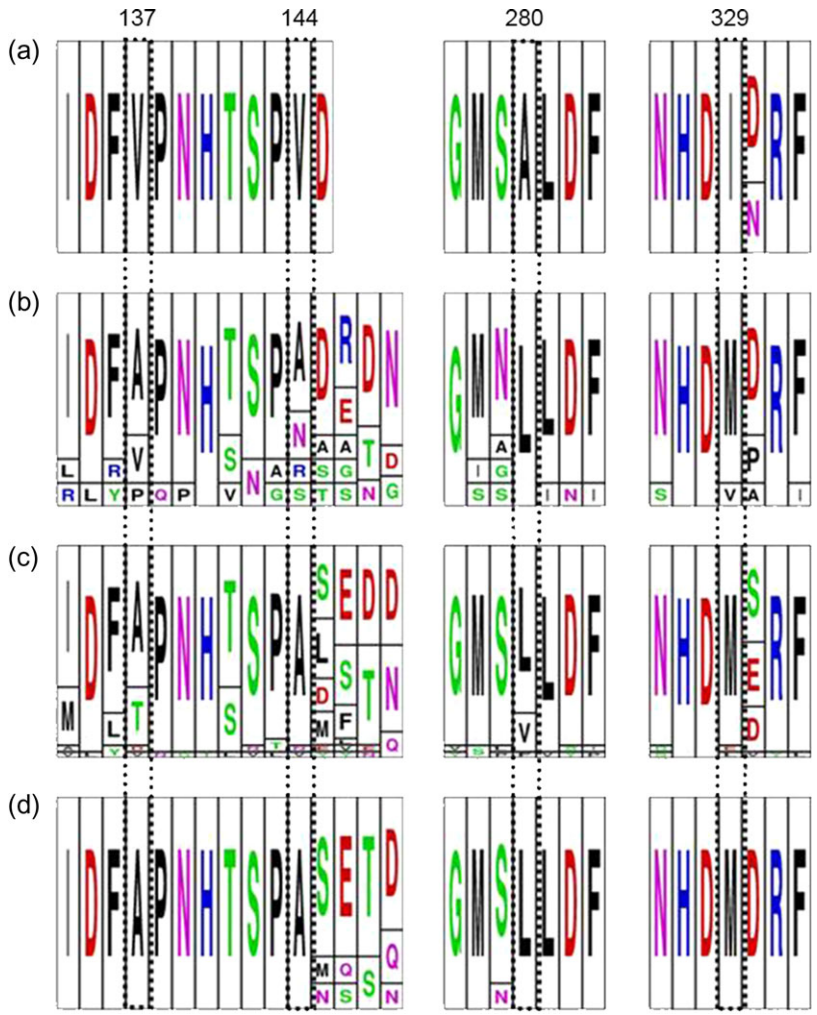

Fig. 1 Logo representation of amino acid composition at positions 137, 144, 280 and 329 of CGTases with experimentally proved activity. CGTases were grouped by their product specificity in 3 γ- (**a**), 9 α- (**b**), 33 β- (**c**) and 8 α/β-CGTases (**d**) according to the CAZy database. Amino acids are indicated in the single-letter code. Letter size represents the frequency of the corresponding residue at each position of the alignment. Amino acid chemical properties: hydrophobic (A, F, I, L, M, P, and V), acid (D and E), basic (H and R), polar (G, S, T and Y) and containing an amide-group (N and Q).

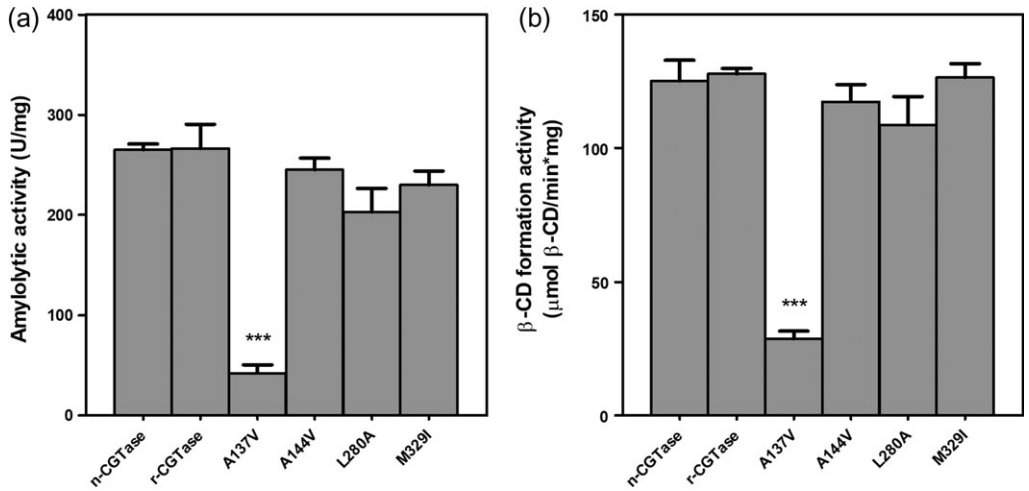

Fig. 2 (**a**) Amylolytic and (**b**) β-cyclizing activity profiles for native CGTase (n-CGTase), recombinant CGTase (r-CGTase) and mutants CGTases carrying single mutations (A137V, A144V, L280A and M329I).

Table II. Kinetic parameters for the β-cyclizing activity of the enzymes under study

CGTase[a]	V_{max} μmol β-CD min^{-1} mg^{-1}	K_m mg ml^{-1}	k_{cat} s^{-1}	k_{cat}/K_m ml mg^{-1} s^{-1}
n-CGTase	189.2 ± 5.8	0.84 ± 0.13	250.4 ± 8.8	298.1 ± 10.1
r-CGTase	191.5 ± 6.9	0.89 ± 0.11	245.3 ± 7.6	275.6 ± 9.8
A137V[b]	20.0 ± 0.5	0.97 ± 0.14	24.8 ± 1.5	25.6 ± 1.1
A144V	185.8 ± 4.8	0.91 ± 0.11	238.2 ± 9.8	262.2 ± 11.3
L280A	147.6 ± 5.6	0.95 ± 0.14	183.9 ± 8.6	193.7 ± 12.6
M329I	186.7 ± 8.5	0.78 ± 0.14	231.6 ± 10.5	296.9 ± 14.5

[a]All determinations were carried out in triplicate. Errors are expressed as standard deviations.
[b]$P < 0.0001$.

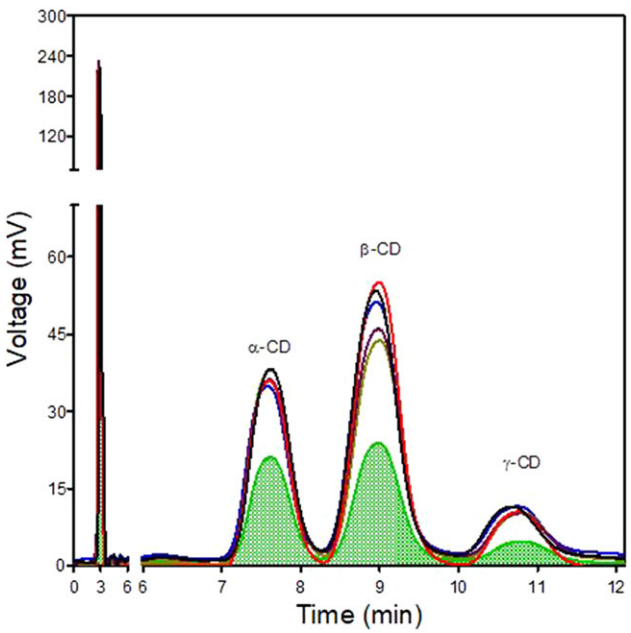

Fig. 3 Production of CD from cassava starch as determined by HPLC. The elution patterns of CD mixtures produced with n-CGTase, r-CGTase, and mutant enzymes A144V, L280A and M329I are indicated by solid lines. Spotted area denotes mutant enzyme A137V.

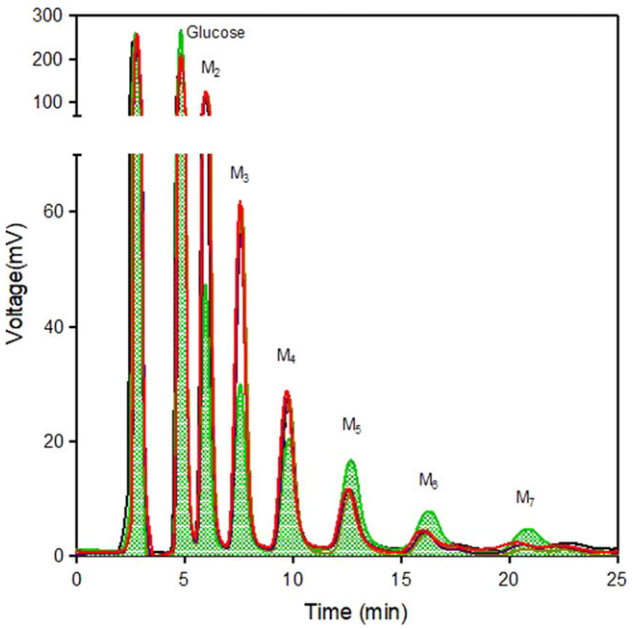

Fig. 4 HPLC elution pattern of MOS production from cassava starch with n-CGTase, r-CGTase and mutant enzymes A144V, L280A and M329I are indicated in solid lines; spotted area denotes mutant enzyme A137V. M2, maltose; M3, maltotriose; M4, maltotetraose; M5, maltopentaose; M6, maltohexaose and M7, maltoheptaose standards.

21.6 mg/ml for mutant A137V and r-CGTase, respectively, $P < 0.0001$). Also, this mutant displayed the lowest yield in MOS production (30.8% versus 47.8% for r-CGTase, $P < 0.0001$) (Figure 4 and Table IV). Interestingly, this mutant increased the proportion of MOS with higher degree of polymerization in the reaction mixture. As shown in Table IV, the content of maltose (M2) and maltotriose (M3) was lower than the yield obtained with the rest of the enzymes, with no changes in maltotetraose (M4) content. Conversely, mutant A137V doubled the proportion of maltopentaose (M5) and maltohexaose (M6) and increased the yield of maltoheptaose (M7) five times as compared to r-CGTases $P < 0.0001$. These results demonstrate the involvement of position 137 in cyclic as well as in linear oligosaccharides production.

Molecular dynamics simulations

To better characterize the impact of the mutated residues at the molecular level, homology-based structural models of wild type and mutant CGTases were obtained. These models were further subjected to molecular dynamics simulations in order to analyze local effects of mutations in terms of their interaction with other amino acids of the catalytic site or with glucose residues of the substrate (Figure 5).

Mutations A144V and M329I did not show any structural variation in the context of the catalytic site of mutant CGTases as compared to n-CGTase (data not shown).

It has been shown that in the n-CGTase residue 280 is located near residue E257, an amino acid of the catalytic triad that in turn contacts the CGTase residue R227 and a glucose residue of the substrate molecule (Glc691). So, we hypothesized that a disruption of the local structure of residue 280 could alter E257 interactions. In fact, the mean distances between E257 and R227 were shortened in mutant L280A (1.90 Å versus 2.53 Å in the n-CGTase), along with a smaller distance fluctuation throughout the simulation period (max.-min: 2.78-1.66 Å and 4.10-1.75 Å for L280A and n-CGTase, respectively). Similarly, the mean distance between E257 and Glc691 was decreased in the mutant (4.13 Å [max.-min: 6.03-1.42 Å] for L280A versus 3.74 Å [max.-min.: 5.75-1.50 Å] for n-CGTase) (Figure 5a and b). Of note, in the latter the distances

Table III. Total quantities and proportions of α-, β-, γ-CD and starch conversion for each CGTase

CGTase	Starch conversion	CD (mg/ml)			
	(%)	Total	α[a]	β	γ
n-CGTase	45.2 ± 3.8	22.6 ± 1.9	7.5 ± 0.6 (33.2)	12.0 ± 1.0 (53.1)	3.1 ± 0.2 (13.7)
r-CGTase	43.2 ± 2.8	21.6 ± 1.8	7.9 ± 0.5 (36.6)	11.0 ± 1.1 (50.9)	2.7 ± 0.2 (12.5)
A137V	22.6 ± 1.9	11.3 ± 1.0	4.2 ± 0.4 (37.2)	5.8 ± 0.5 (51.3)	1.3 ± 0.1 (11.5)
A144V	43.0 ± 3.4	21.5 ± 1.7	7.8 ± 0.7 (36.3)	11.0 ± 0.9 (51.2)	2.7 ± 0.2 (12.6)
L280A	42.6 ± 3.5	21.3 ± 1.8	7.4 ± 0.6 (34.7)	11.0 ± 0.9 (51.6)	2.9 ± 0.3 (13.6)
M329I	49.8 ± 4.0	24.9 ± 2.0	7.7 ± 0.6 (30.9)	14.0 ± 1.1 (56.2)	3.2 ± 0.2 (12.9)

[a]Numbers between brackets indicate the percentage of each type of CD in the product mixture.

Table IV. Total quantities and proportions of MOS and starch conversion for each CGTase

CGTase	Starch conversion	MOS (mg/ml)					
	(%)	M2[a]	M3	M4	M5	M6	M7
n-CGTase	48.8 ± 1.8	21.0 ± 0.7 (43.0)	13.1 ± 1.1 (26.8)	8.1 ± 0.7 (16.6)	3.4 ± 0.4 (7.0)	2.2 ± 0.6 (4.5)	1.0 ± 0.5 (2.1)
r-CGTase	47.8 ± 1.6	20.0 ± 0.7 (41.8)	12.8 ± 1.1 (26.8)	7.5 ± 0.7 (15.7)	4.0 ± 0.4 (8.4)	2.7 ± 0.6 (5.6)	0.8 ± 0.2 (1.7)
A137V	30.8 ± 1.8	8.1 ± 1.0 (26.3)	6.3 ± 0.3 (20.5)	4.7 ± 0.1 (15.3)	5.0 ± 1.1 (16.2)	3.9 ± 0.1 (12.7)	2.8 ± 0.5 (9.0)
A144V	44.1 ± 1.4	19.4 ± 0.9 (44.0)	12.5 ± 0.4 (28.3)	6.3 ± 0.7 (14.3)	3.2 ± 0.2 (7.3)	1.9 ± 0.3 (4.3)	0.8 ± 0.4 (1.8)
L280A	45.1 ± 1.0	18.7 ± 1.8 (41.5)	11.8 ± 0.7 (26.2)	7.4 ± 0.2 (16.4)	3.0 ± 0.4 (6.7)	3.3 ± 0.2 (7.2)	0.9 ± 0.4 (2.0)
M329I	45.8 ± 1.1	19.9 ± 0.6 (43.5)	12.7 ± 1.1 (27.7)	6.6 ± 1.2 (14.4)	3.6 ± 0.3 (7.9)	1.9 ± 0.3 (4.1)	1.1 ± 0.2 (2.4)

[a]M2, maltose; M3, maltotriose; M4, maltotetraose; M5, maltopentaose; M6, maltohexaose and M7, maltoheptaose. Numbers between brackets indicate the percentage of each type of MOS in the product mixture.

between residues showed increased fluctuation throughout the simulation period.

In turn, no direct effects of mutation A137V on the position of the residues of the catalytic triad were predicted, whereas an indirect effect on H140 was evidenced. Actually, as shown in Figure 5c and d, the mean distance between residues H140 and its interacting residue D229 increased 2.017 times in the mutant enzyme when compared with n-CGTase (3.82 Å [max.-min.: 5.33-3.01 Å] versus 1.90 Å [max.-min.: 3.57-1.62 Å]). Additionally, the RMSD plot of Glc691 of the substrate molecule in the n-CGTase and in the L280A and A137V mutants along simulation did not show differences (Supplementary Figure S1).

Together, these results provide molecular evidence of the contribution of residues L280 and A137 in the enzymatic activity of the CGTase of *P. barengoltzii*.

Discussion

Many efforts have been made to understand the catalytic mechanism and product specificity of CGTases through protein engineering (Leemhuis *et al*., 2010; Li *et al*., 2016; Wang *et al*., 2016). Because of the industrial use of γ-CD, obtaining this CD has been, and remains to be, one of the main goals of research in this area. Sequence alignment and detailed analysis of CGTase sequences indicate that there are differences between the γ-CGTases and the α- and β-CGTases in two regions that may be involved in product specificity (Leemhuis *et al*., 2010). The first region (145–152; as referred to *B. circulans* 251 CGTase) has been identified at subsite −7. The second region has been identified at subsite −3, which is composed of residues 47 and 87–94. The results obtained after performing different amino acid replacements in these regions suggest that more space for the binding of the glycosyl chain is needed for a higher level of γ-cyclization activity (Li *et al*., 2007; Wang *et al*., 2016). In this work, we selected four additional positions that differ between γ- and α- and β-CGTases which had not been individually evaluated before. These positions were studied because of their proximity to the active site subsites. Unfortunately, our hypothesis that the introduction of single γ-CGTase residues into the active site of the α/β-CGTase from strain DF 9 R could enhance γ-cyclodextrin production was not supported by experimental results. Nevertheless, a collective role of these residues affecting enzyme selectivity and producing diverse proportions of CDs cannot be ruled out.

Two mutations proved to affect the interaction between the catalytic site and the substrate. In fact, mutant L280A showed less catalytic efficiency than r-CGTase, probably due to spatial changes between E257 and residues R227 and Glc691, as demonstrated by molecular dynamics simulation. Interestingly, Wang *et al*. (2017) showed that mutation of the conserved residue R277 of the CGTase from *Bacillus* sp. N-222 led to an enhanced activity of this enzyme, thus supporting the relevance of this residue. In turn, mutation of residue A137 demonstrated that this amino acid is essential for the amylolytic and β-CD formation activities, thus contributing to the structure-function relationship of this important group of enzymes.

Due to the magnitude of the observed changes in enzymatic activities, mutant A137 deserves particular analysis. Alanine has a relative accessible surface area (Tien *et al*., 2013), lower than that of valine (121Å^2 and 165 Å^2, respectively); moreover, its hydrophobicity is lower according to the Kyte and Doolittle scale (+1.8 versus +4.2) (Kyte and Doolittle, 1982). The molecular dynamics simulations indicate that these bulk and hydrophobicity differences produce changes in the catalytic site of the enzyme, resulting in a displacement of H140 which moves away from the catalytic D229 (Figure 5). As a result, the distance D229-H140 was 2.017-fold higher in the A137V mutant than in the wild type enzyme. Residue H140, which is located in the subsite -1 of substrate binding, is

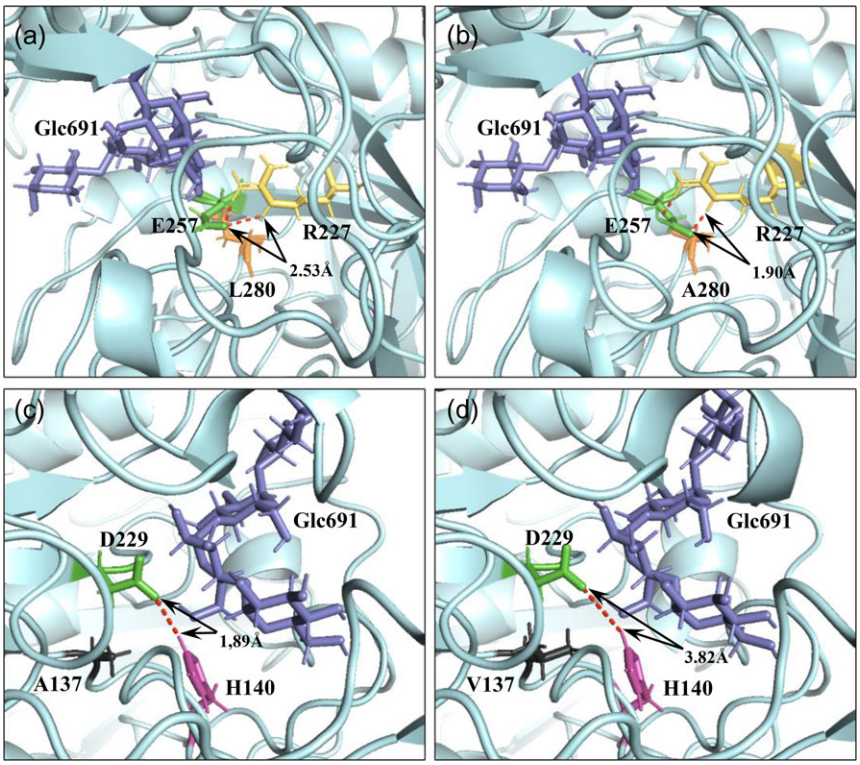

Fig. 5 Structural comparison of the catalytic site of n-CGTase from *P. barengoltzii* in the environment of position 280 (**a**) and 137 (**c**) and mutants L280A (**b**) and A137V (**d**) after a molecular dynamics simulation of 20 ns. Hydrogen bonds are shown with dotted lines. The distances between arrows correspond to the separation between R227 and E257 (**a**, **b**) and between H140 and D229 (**c**, **d**). The crystal structure of *Bacillus circulans* 251 strain (PDB 1CXH) was used as the template.

conserved in CGTases and favors the formation of the required positive charge in the transition state during enzymatic catalysis (Uitdehaag *et al.*, 1999). It is likely that an adequate stabilization of the transition state does not occur in mutant A137V with the consequent decrease of enzymatic activity. This alteration did not change the affinity of the enzyme towards the substrate (the K_m values of native and mutant enzymes were similar) but caused a drastic 10-fold decrease in k_{cat}, and thus in catalytic efficiency.

Strikingly, mutant A137V produced a significant increase in the amount of highly polymerized MOS as compared to r-CGTase, mainly maltopentaose (2x), maltohexaose (2x) and maltoheptaose (5x). Other authors have studied the role of specific residues of the maltohexaose-producing amylase from alkalophilic *Bacillus* sp. 707 in M6 production. In particular, a hydrophobic residue like tryptophan at position 133 would facilitate a strong interaction between the catalytic subsite of this amylase and the glycosyl residue which would enhance M6 production (Kanai *et al.*, 2004). Since this maltohexaose-producing amylase and CGTases belong to the same enzyme family, it seems plausible that the increased production of high-degree polymerization MOS is favored also by hydrophobic residues in CGTases. In fact, the CGTase of *P. barengoltzii* strain DF 9 R shows an isoleucine residue at position 133. Moreover, the distance between residue 137 and other residues around the subsites interacting with the glycosyl residues of the oligosaccharide produced including residue 133 decreased in the A137V mutant as compared to the n-CGTase (data not shown). Thus, the introduction of a valine residue at position 137 would contribute to a more hydrophobic environment leading to the preferential production of high-degree polymerization MOS.

Maltooligosaccharides can be produced from starch mainly by glycosyl hydrolases. These enzymes use inexpensive and easy to get saccharides such as starch as substrates for MOS production. In particular, α-amylase (EC 3.2.1.1) randomly cleaves the α-1,4 glycosidic linkages of starch to yield a mixture of maltodextrin, MOS and glucose. Other hydrolytic enzymes preferentially produce a particular type of MOS from starch; they are collectively known as maltooligosaccharide-forming amylases (MFAses) (Pan *et al.*, 2017). MFAses emerge as a promising biotechnological tool given their ability to produce mainly a single type of MOS. MFAses include maltotriose forming amylase (G3-amylase; EC 3.2.1.116), maltotetraose-forming amylase (G4-amylase; EC 3.2.1.60), maltopentaose-forming amylase (G5-amylase; EC 3.2.1.-) and maltohexaose forming amylase (G6-amylase; EC 3.2.1.98) (Pan *et al.*, 2017). Additionally, different α-amylases may be used in combination with debranching enzymes such as pullulanase (EC 3.2.1.41) and isoamylase (EC3.2.1.68) to produce MOS from starch. In this case, the length of the MOS obtained depends on the α-amylase used (Doukyu *et al.*, 2007).

As mentioned before, CGTases catalyze starch hydrolysis as well as disproportionation reactions that lead to MOS production. In this work, mutation of the CGTase from *P. barengoltzii* strain DF 9 R at position 137 led to the preferential production of MOS with higher degree of polymerization. It is worth mentioning that under the experimental conditions used this reaction occurred by disproportionation with negligible production of CD, as demonstrated previously by Rodríguez Gastón *et al.* (2012). To our knowledge, this is the first report of a recombinant CGTase that produces an enrichment of high-polymerization degree MOS by disproportionation.

Future studies on the molecular mechanisms involved in the product specificity of this CGTase will lead to the rational design of recombinant enzymes that may be employed in specific MOS production.

Supplementary Data

Supplementary data are available at *Protein Engineering, Design and Selection* online.

Acknowledgments

We thank María Inés Gismondi for language supervision. H.C. and O.A.T. are career members of the Argentine Council of Scientific and Technical Research (CONICET). JdlMC is a PhD student from the Scientific Research Commission of the Province of Buenos Aires (CIC). SCL is PhD student from Universidad Nacional de Luján. A generous allocation of computing time at the Scientific Computation Center of the UAM (CCC-UAM) and an institutional grant from Fundación Ramón Areces to CBMSO are also acknowledged.

Funding

This work was supported by Agencia Nacional de Promoción Científica y Tecnológica [PICT 2013-0880, PICT 2016-0240], Universidad Nacional de Luján, and project BIO2013-4496R from the Spanish Ministry of Economy and Competitiveness.

References

Ban,X., Gu,Z., Li,C., Huang,M., Cheng,L., Hong,Y. and Li,Z. (2015) *Int. J. Biol. Macromol.*, **76**, 224–229.

Basso,F.M., Mangolim,C.S., Aguiar,M.F.A., Monteiro,A.R.G., Peralta,R.M. and Matioli,G. (2015) *Int. J. Food Sci. Nutr.*, **66**, 275–281.

Bradford,M.M. (1976) *Anal. Biochem.*, **72**, 248–254.

Costa,H., Distéfano,A.J., Marino-Buslje,C., Hidalgo,A., Berenguer,J., Biscoglio De Jiménez Bonino,M. and Ferrarotti,S.A. (2012) *Appl. Microbiol. Biotechnol.*, **94**, 123–130.

Costa,H., Gastón,J.R., Lara,J., Martinez,C.O., Moriwaki,C., Matioli,G. and Ferrarotti,S.A. (2015) *Bioprocess Biosyst. Eng.*, **38**, 1055–1063.

Crooks,G.E., Hon,G., Chandonia,J.M. and Brenner,S.E. (2004) *Genome Res.*, **14**, 1188–1190.

Doukyu,N., Yamagishi,W., Kuwahara,H., Ogino,H. and Furuki,N. (2007) *Extremophiles*, **11**, 781–788.

Ferrarotti,S.A., Rosso,A.M., Maréchal,M.A., Krymkiewicz,N. and Maréchal, L.R. (1996) *Cell Mol. Biol. (Noisy-le-Grand, France)*, **42**, 653–657.

Goel,A. and Nene,S.N. (1995) *Starch—Stärke*, **47**, 399–400.

Goh,K.M., Mahadi,N.M., Hassan,O., Rahman,R.N.Z.R.A. and Illias,R.M. (2009) *J. Mol. Catal. B: Enzym.*, **57**, 270–277.

Green,M.R., Sambrook,J. and Sambrook,J. (2012) *Molecular Cloning: A Laboratory Manual*. Cold Spring Harbor Laboratory Press, Cold Spring Harbor, N.Y.

Han,R., Li,J., Shin,H.D., Chen,R.R., Du,G., Liu,L. and Chen,J. (2014) *Biotechnol. Adv.*, **32**, 415–428.

Huang,M., Li,C., Gu,Z., Cheng,L., Hong,Y. and Li,Z. (2014) *J. Agric. Food Chem.*, **62**, 11209–11214.

Kanai,R., Haga,K., Akiba,T., Yamane,K. and Harata,K. (2004) *Biochem.*, **43**, 14047–14056.

Kelly,R.M., Leemhuis,H., Rozeboom,H.J., van Oosterwijk,N., Dijkstra,B.W. and Dijkhuizen,L. (2008) *Biochem. J.*, **413**, 517–525.

Knegtel,R.M., Strokopytov,B., Penninga,D., Faber,O.G., Rozeboom,H.J., Kalk,K.,.H., Dijkhuizen,L. and Dijkstra,B.W. (1995) *J. Biol. Chem.*, **270**, 29256–29264.

Kurkov,S.V. and Loftsson,T. (2013) *Int. J. Pharm.*, **453**, 167–180.

Kyte,J. and Doolittle,R.F. (1982) *J. Mol. Biol.*, **157**, 105–132.

Laemmli,U.K. (1970) *Nature*, **227**, 680–685.

Leemhuis,H., Kelly,R.M. and Dijkhuizen,L. (2010) *Appl. Microbiol. Biotechnol.*, **85**, 823–835.

Li,Z.F., Zhang,J.Y., Sun,Q., Wang,M., Gu,Z.B., Du,G.C., Wu,J. and Chen,J. (2009a) *J. Agric. Food Chem.*, **57**, 8386–8391.

Li,Z., Chen,S., Gu,Z., Chen,J. and Wu,J. (2014) *Trends Food Sci. Technol.*, **35**, 151–160.

Li,Z., Gu,Z., Wang,M., Du,G., Wu,J. and Chen,J. (2010) *Appl. Microbiol. Biotechnol.*, **85**, 553–561.

Li,Z., Huang,M., Gu,Z., Holler,T.P., Cheng,L., Hong,Y. and Li,C. (2016) *Int. J. Biol. Macromol.*, **83**, 111–116.

Li,Z., Wang,M., Wang,F., Gu,Z., Du,G., Wu,J. and Chen,J. (2007) *Appl. Microbiol. Biotechnol.*, **77**, 245.

Li,Z., Zhang,J., Wang,M., Gu,Z., Du,G., Li,J., Wu,J. and Chen,J. (2009b) *Appl. Microbiol. Biotechnol.*, **83**, 483–490.

Lombard,V., Golaconda Ramulu,H., Drula,E., Coutinho,P.M. and Henrissat, B. (2014) *Nucleic Acids Res.*, **42**, D490–D495.

Pan,S., Ding,N., Ren,J., Gu,Z., Li,C., Hong,Y., Cheng,L., Holler,T.P. and Li, Z. (2017) *Biotechnol. Adv.*, **35**, 619–632.

Rodríguez Gastón,J.A., Costa,H., Rossi,A.L., Krymkiewicz,N. and Ferrarotti, S.A. (2012) *Process Biochem.*, **47**, 2562.

Rosso,A.M., Ferrarotti,S.A., Krymkiewicz,N. and Nudel,B.C. (2002) *Microb. Cell Factories*, **1**, 3–3.

Rostinawati,T., Riani,C., Elfahmi,E., Sumirtapura,Y.C. and Retnoningrum,D. S. (2015) *Biotechnol.*, **14**, 181–187.

Stam,M.R., Danchin,E.G., Rancurel,C., Coutinho,P.M. and Henrissat,B. (2006) *Protein Eng. Des. Sel.*, **19**, 555–562.

Szerman,N., Schroh,I., Rossi,A.L., Rosso,A.M., Krymkiewicz,N. and Ferrarotti,S.A. (2007) *Bioresour. Technol.*, **98**, 2886–2891.

Thompson,J.D., Gibson,T.J., Plewniak,F., Jeanmougin,F. and Higgins,D.G. (1997) *Nucleic Acids Res.*, **25**, 4876–4882.

Tien,M.Z., Meyer,A.G., Sydykova,D.K., Spielman,S.J. and Wilke,C.O. (2013) *PLoS One*, **8**, e80635.

Uitdehaag,J.C.M., Kalk,K.H., van der Veen,B.A., Dijkhuizen,L. and Dijkstra, B.W. (1999) *J. Biol. Chem.*, **274**, 34868–34876.

Van Der Maarel,M.J.E.C. and Leemhuis,H. (2013) *Carbohydr. Pol.*, **93**, 116–121.

van der Veen,B.A., Uitdehaag,J.C.M., Dijkstra,B.W. and Dijkhuizen,L. (2000) *Mol. Enzymol*, **1543**, 336–360.

Wang,H., Zhou,W., Li,H., Rie,B. and Piao,C. (2017) *3 Biotech.*, **7**, 149.

Wang,L., Duan,X. and Wu,J. (2016) *Appl. Environ. Microbiol.*, **82**, 2247–2255.

Wang,L., Wu,D., Chen,J. and Wu,J. (2013) *Food Chem.*, **141**, 3072–3076.

Wu,D., Chen,S., Wang,N., Chen,J. and Wu,J. (2012) *Appl. Biochem. Biotechnol.*, **167**, 1954–1962.

Xie,T., Hou,Y., Li,D., Yue,Y., Qian,S. and Chao,Y. (2014a) *J. Biotechnol.*, **182–183**, 92–96.

Xie,T., Song,B., Yue,Y., Chao,Y. and Qian,S. (2014b) *J. Biotechnol.*, **170**, 10–16.